Synthesis and structure of triple thorium phosphates with monazite structure

Alexander Knyazev[1] · Ivan Savushkin[1] · Ulmas Mirsaidov[1,2] · Alexey Lukoyanov[1] · Artem Oganov[1,3]

Abstract

Three monazites $M_{II}LaTh(PO_4)_3$ (M_{II} = Ca, Sr, Cd) have been studied both computationally and experimentally to determine the influence of the M_{II} cation nature on monazite crystal structure and characteristics important for their use as matrix forms for immobilizing radioactive waste. Their crystal structures have been refined by the Rietveld method. Functional composition has been confirmed by IR spectroscopy. Thermal stability has been tested by DTA-TG.

Keywords Monazite · Thorium phosphate, $M_{II}LaTh(PO_4)_3$ · Crystal structure · Rietveld method · IR spectroscopy

Introduction

The safest way to dispose of nuclear waste is to bury it in deep geological formations. The introduction of radionuclides into the crystalline structure of minerals is used for immobilization of radioactive waste. This matrix does not undergo destruction and amorphization, so the development of such crystalline structures is an urgent task [1].

Compounds with a monazite structure are suitable for this task due to their chemical, thermal and radiation stability, as well as low coefficients of thermal expansion.

Monazite is a rather rare mineral and, as a rule, found in the form of an admixture of granite igneous and gneiss metamorphic rocks [2]. This mineral is prone to isovalent and heterovalent isomorphism, therefore it is likely to include various rare earth and alkaline earth elements, as well as actinides that can replace cerium.

Various monazites contain lanthanides (La > Nd > Pr > Sm > Gd) in the form of constant isomorphic impurities that replace Ce in a 1:1 ratio. An impurity of cerophosphorhuttonite $ThCeSiPO_8$, which is essentially an intermediate between monazite and huttonite, was also found in monazites. This mineral is isostructural to monazite. Significant amounts of other elements are also found in natural monazites: Th (up to 32%), Si (up to 6.1%), Y (up to 5.1%), U (up to 6.6%), Ca (up to 6%) and S (up to 3%). This gives us a reason to suppose that lanthanides in the oxidation state of 3+ (cerium, samarium, europium, gadolinium), actinides in the oxidation state of 4+ (thorium, uranium, neptunium, plutonium) and cerium (4+) can be simultaneously involved in monazite-like phosphate compounds [3, 4].

In this work, 3 new phosphates $CaLaTh(PO_4)_3$, $SrLaTh(PO_4)_3$, $CdLaTh(PO_4)_3$ are investigated. These compounds can be considered as an example of the binding of the lanthanide-actinide fraction of spent nuclear fuel into a single crystalline matrix [5].

Experiment

Synthesis of triple phosphates type $M_{II}LaTh(PO_4)_3$.

Solid state synthesis was used for preparation $M_{II}LaTh(PO_4)_3$. Oxides and salts of the chemically pure class were used as reagents: lanthanum oxide La_2O_3, bivalent metal nitrates $Ca(NO_3)_2$, $Sr(NO_3)_2$, $Cd(NO_3)_2$, thorium nitrate crystalline hydrate $Th(NO_3)_4 \cdot 5H_2O$ and ammonium dehydrogen phosphate $NH_4H_2PO_4$ [5]. The starting reagents were mixed according to the stoichiometry of the resulting solid compounds. Mixtures of powders were thoroughly milled in an agate mortar and placed in an oven. The solid solutions were heated at a heating rate of 5 K min^{-1} to 773 K

✉ Alexander Knyazev
  knyazevav@gmail.com

1 Lobachevsky University, Gagarin Prospekt 23/2, Nizhny Novgorod, Russia 603950

2 Nuclear and Radiation safety Agency, Hamza Hakimzoda Street 17 A, 734025 Dushanbe, Republic of Tajikistan

3 Skolkovo Institute of Science and Technology, Bolshoy Boulevard 30, bld. 1, Moscow, Russia 121205

and held for 2 h to anneal the nitrates. Then, the samples were again milled and additionally heated at 1550 K for 12 h. The resulting white powders were carefully milled in an agate mortar for further analysis.

X-ray diffraction

The obtained samples were characterized with a Shimadzu XRD-6000 X-ray diffractometer using CuK_α radiation ($\lambda = 1.5406$ Å), in which 2θ scans from 10° to 120° with a step width of 0.02° were recorded [6–8]. To clarify the structure of the obtained compounds, the observed diffraction data were analyzed using the Bruker Topas 3 program [9], the background parameters were corrected by a sixth order polynomial and the corresponding scaling factor.

$LaPO_4$ structure with the space group $P2_1/n$ was used as the original model to refine the structures obtained compounds [10]. Reflex profiles were approximated by the pseudo-Voigt function. The refinement of the crystal structures was carried out by successively increasing the determined parameters until the R factor stabilized; as a result, the unit cell parameters, the coordinates of the basic atoms, and their population were determined.

The structure decoding data are shown in Table 1. The calculated and experimental X-ray diffraction spectra of thorium phosphates are shown in Fig. 1. The atomic coordinates and cation occupancy are given in Tables 2, 3 and 4.

The structures of all three compounds are similar and constitute a dense framework (Fig. 2) in based on 14-sided $MetO_9$ deltahedrons (where Met = Ca, Sr, Cd, Th, La) and phosphate tetrahedra PO_4 (Fig. 3) which are connected by mono and bidentant oxygen atoms.

In all the compounds obtained, the $MetO_9$ deltahedra and the PO_4 tetrahedra are distorted (Fig. 4); when comparing the Met–O bond lengths, it can be noted that in

$SrLaTh(PO_4)_3$ the distortion is minimal; when comparing the P–O bond lengths, $CdLaTh(PO_4)_3$ underwent the greatest distortion, which is confirmed by the IR spectroscopy.

The unit cell parameters of all the obtained $CaLaTh(PO_4)_3$ $SrLaTh(PO_4)_3$ $CdLaTh(PO_4)_3$ compounds are less than that of $La(PO_4)_3$ with the monazite structure that was taken as the original model. Moreover, one can trace such a tendency that the greater the distortion of the structure, the smaller the volume and other parameters of the unit cell. The change in the size of the structure can be explained by a change in the ionic radius of the metals that make up the compounds obtained, where in addition to Th and La there are Ca, Sr, and Cd, the radii of which differ r (Sr) = 1.12Å > r (Ca) = 0.99Å > r (Cd) = 0.97 Å. Thus, the larger the ionic radius of the divalent metal, the less distortion of the structure of the obtained monazite.

IR-spectroscopy

The functional composition was confirmed using an FTIR-8400S FTIR spectrophotometer from Shimadzu. To record the IR spectrum in the wave numbers of 1600–400 cm^{-1} and the studied samples were prepared in the form of tablets with KBr [5]. IR spectra were recorded with an accuracy of determining the absorption of maxima of $\pm$ (0.1–0.2) cm^{-1}. The spectra obtained are plotted on Fig. 5.

The IR spectrum is generally similar to cerium orthophosphate [12], which indicates that the studied compounds are monazites. However, in the region of asymmetric stretching vibrations ν_3 (1280–1020 cm^{-1}), there are no distinct bands characteristic of cerium phosphate. The IR spectra in this range of wave numbers are blurred and barely noticeable maxima can be seen in $SrLaTh(PO_4)_3$, this indicates a random arrangement of cations in equivalent positions of the crystal structure of the obtained monazites. In the region of bending vibrations (645–430 cm^{-1}), the splitting of 2 bands characteristic of phosphates is observed. This is due to the distortion of the phosphate tetrahedron, which is especially pronounced in the spectrum of $CdLaTh(PO_4)_3$.

Thermal stability

Setaram LABSYS TG-DTA/DSC 1600 at a speed and cooling of 0.1667 K s^{-1} in an argon atmosphere. Platinum crucibles are used in experiments. All sizes of the compound correspond. The samples were heated from 30 to 1200 °C. In this temperature range, neither decay processes nor phase transitions are observed (Fig. 6). This is due to the tight packaging.

Table 1 Intensity data collection conditions and structure refinement results for monazite phosphate

Sample	$CaLaTh(PO_4)_3$	$SrLaTh(PO_4)_3$	$CdLaTh(PO_4)_3$
a (Å)	6.7420 (2)	6.8037 (1)	6.7226 (2)
b (Å)	6.9567 (2)	7.0313 (1)	6.9392 (2)
c (Å)	6.4405 (2)	6.5071 (1)	6.4158 (1)
beta	103.582 (2)	103.436 (1)	103.840 (2)
V (Å3)	293.62 (2)	302.77 (1)	290.61 (1)
ρ (g/cm3)	5.2474 (3)	5.4364 (2)	5.8528 (3)
U	0.194 (2)	− 0.0032 (36)	− 0.230 (11)
V	− 0.099 (1)	0.022 (3)	0.219 (10)
W	0.0394 (3)	− 0.00675 (86)	− 0.0456 (21)
Rwp	4.866	5.852	5.802
Space group	$P2_1/n$	$P2_1/n$	$P2_1/n$
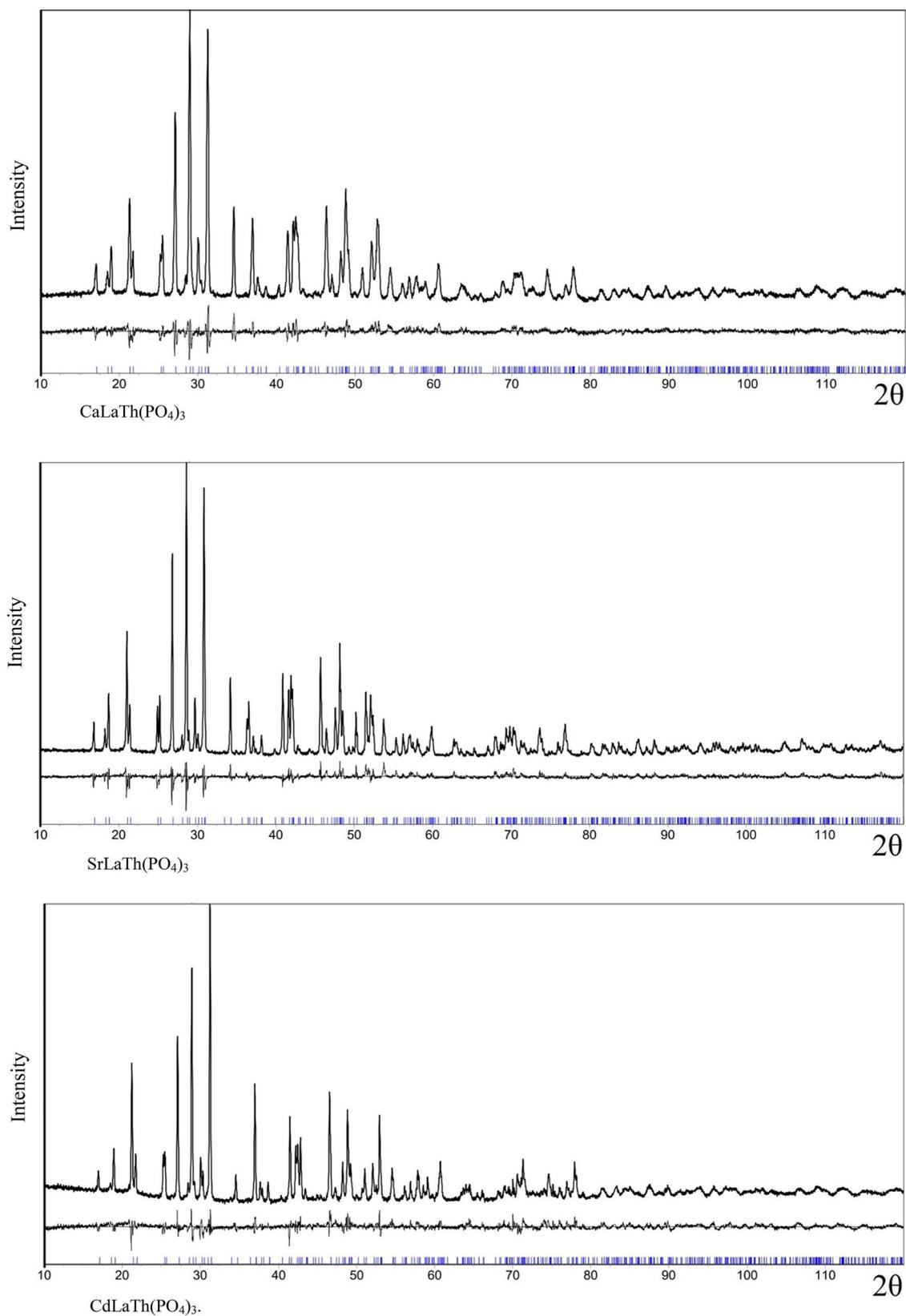
Fig. 1 The calculated, experimental profiles (upper curves) and difference X-ray diffraction patterns (bottom curve) for the compounds $CaLaTh(PO_4)_3$, $SrLaTh(PO_4)_3$, $CdLaTh(PO_4)_3$. Reflection positions are presented by vertical hash marks

Table 2 The atomic coordinates for $CaLaTh(PO_4)_3$

Atom	Occ	x	y	z
Ca	0.3333	0.28091 (26)	0.33746 (35)	0.10213 (34)
La	0.3333	0.28091 (26)	0.33746 (35)	0.10213 (34)
Th	0.3333	0.28091 (26)	0.33746 (35)	0.10213 (34)
P	1	0.3035 (11)	0.3331 (12)	0.6131 (12)
O(1)	1	0.1245 (21)	0.3036 (20)	0.7082 (23)
O(2)	1	0.2454 (21)	0.4869 (23)	0.4484 (25)
O(3)	1	0.4749 (18)	0.3819 (20)	0.7942 (19)
O(4)	1	0.3736 (18)	0.1811 (24)	0.5176 (23)

Table 3 The atomic coordinates for $SrLaTh(PO_4)_3$

Atom	Occ	x	y	z
Sr	0.3333	0.21714 (29)	0.33783 (34)	0.40073 (35)
La	0.3333	0.21714 (29)	0.33783 (34)	0.40073 (35)
Th	0.3333	0.21714 (29)	0.33783 (34)	0.40073 (35)
P	1	0.1986 (13)	0.3334 (14)	0.8930 (13)
O(1)	1	0.2340 (25)	-0.0194 (26)	0.4329 (30)
O(2)	1	0.4781 (20)	0.8685 (24)	0.7929 (21)
O(3)	1	0.1204 (22)	0.1915 (25)	0.9918 (25)
O(4)	1	0.3683 (24)	0.3015 (21)	0.7880 (26)

Table 4 The atomic coordinates for $CdLaTh(PO_4)_3$

Atom	Occ	x	y	z
Cd	0.3333	0.28117 (31)	0.33903 (37)	0.10369 (29)
La	0.3333	0.28117 (31)	0.33903 (37)	0.10369 (29)
Th	0.3333	0.28117 (31)	0.33903 (37)	0.10369 (29)
P	1	0.2797 (16)	0.3313 (15)	0.5962 (16)
O(1)	1	0.0760 (29)	0.3593 (29)	0.7462 (28)
O(2)	1	0.2359 (36)	0.5164 (32)	0.4124 (35)
O(3)	1	0.5261 (26)	0.3634 (29)	0.8211 (24)
O(4)	1	0.3558 (30)	0.2192 (25)	0.4782 (39)
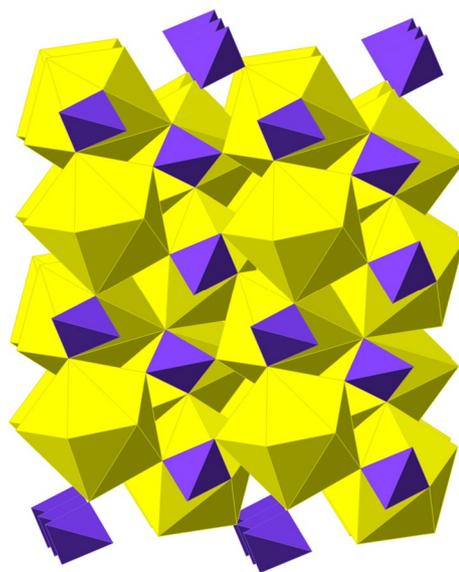
Fig. 2 An example of a dense framework formed by triple phosphates

Conclusions

Triple thorium phosphates have a framework structure. Where the MII, La, and Th atoms occupy the same crystallographic position. The framework is built of 14-sided ThO_9 deltahedrons and PO_4 tetrahedrons that are connected to each other along edges and vertices.

When refining the structure by the Rietveld method, it turned out that the unit cell parameters increase and the distortion decreases in the series $CdLaTh(PO_4)_3 <$ $CaLaTh(PO_4)_3 < SrLaTh(PO_4)_3$. This regularity is due to an increase in the ionic radius in the series $Cd < Ca < Sr$ (0.97 Å, 0.99 Å, 1.12 Å, respectively) that was further confirmed by IR spectroscopy.
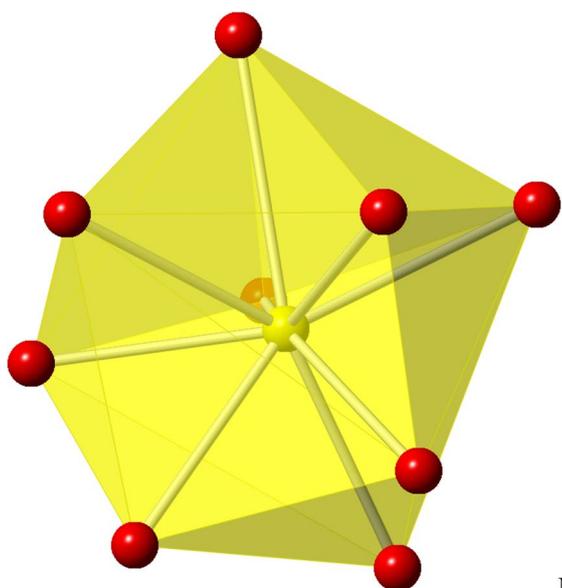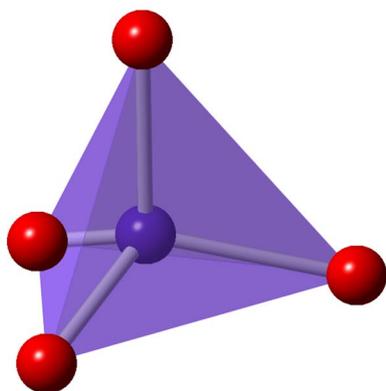
Fig. 3 An example 14-sided $MetO_9$ deltahedron (Met = Ca, Sr, Cd, Th, La) и and phosphate tetrahedra PO_4
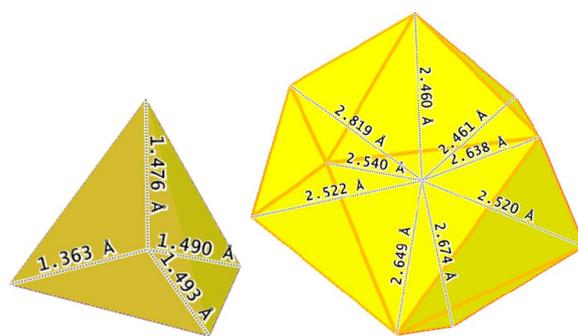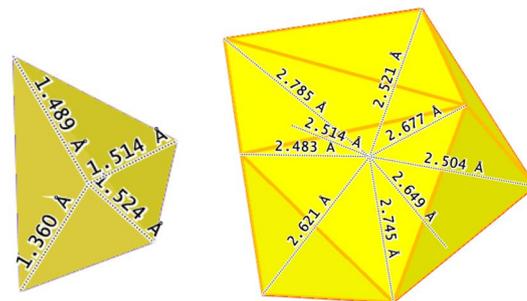
$CaLaTh(PO_4)_3$
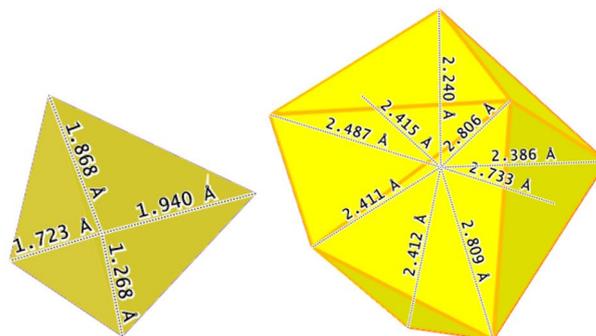
$SrLaTh(PO_4)_3$

$CdLaTh(PO_4)_3$.

Fig. 4 Distorted polyhedra for the resulting compounds $CaLaTh(PO_4)_3$, $SrLaTh(PO_4)_3$, $CdLaTh(PO_4)_3$

Fig. 5 The IR spectra obtained for the compounds $CaLaTh(PO_4)_3$, $SrLaTh(PO_4)_3$, $CdLaTh(PO_4)_3$
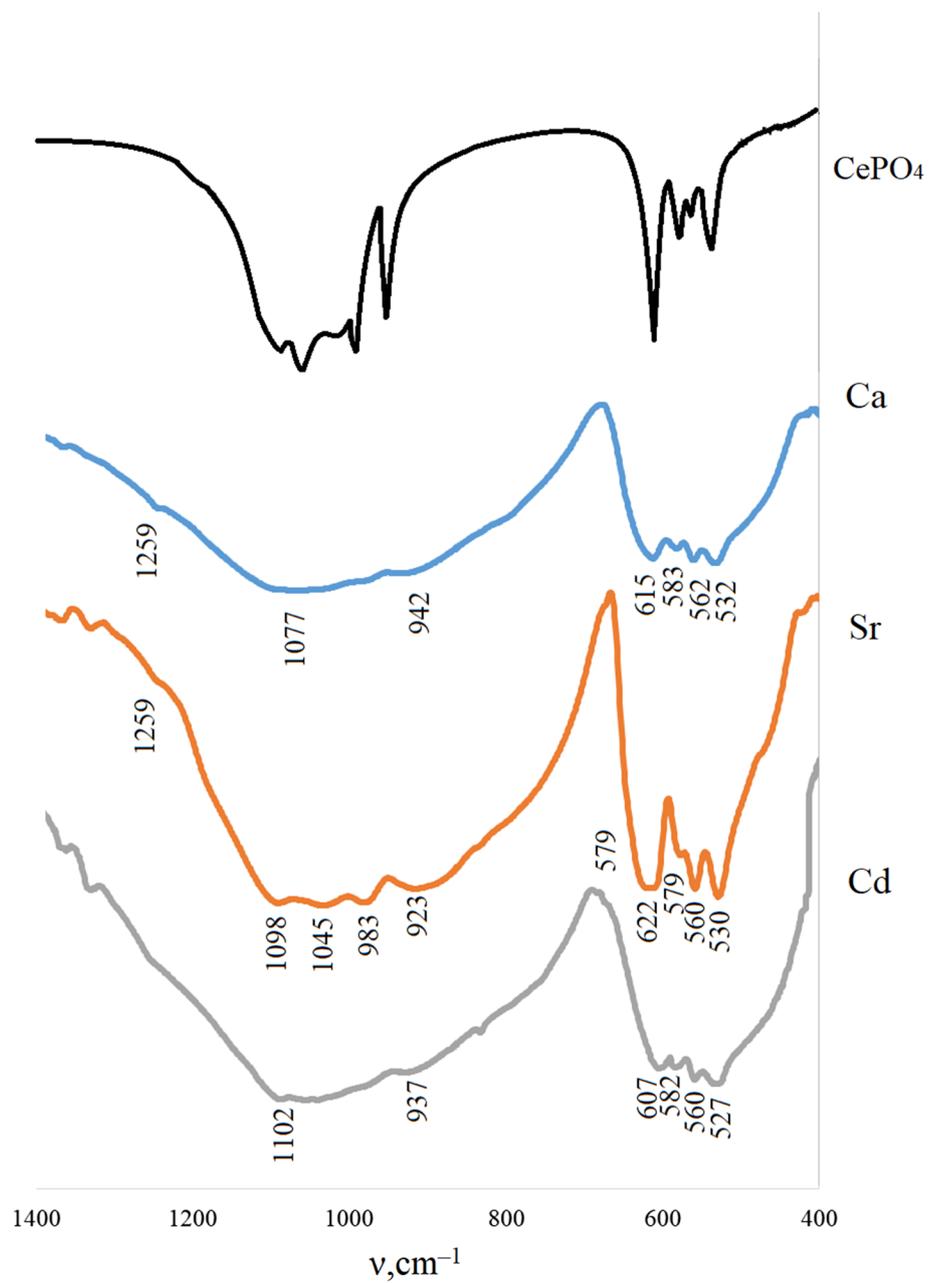
Fig. 6 DSC and TG analysis of compounds CaLaTh(PO$_4$)$_3$, SrLaTh(PO$_4$)$_3$, CdLaTh(PO$_4$)$_3$
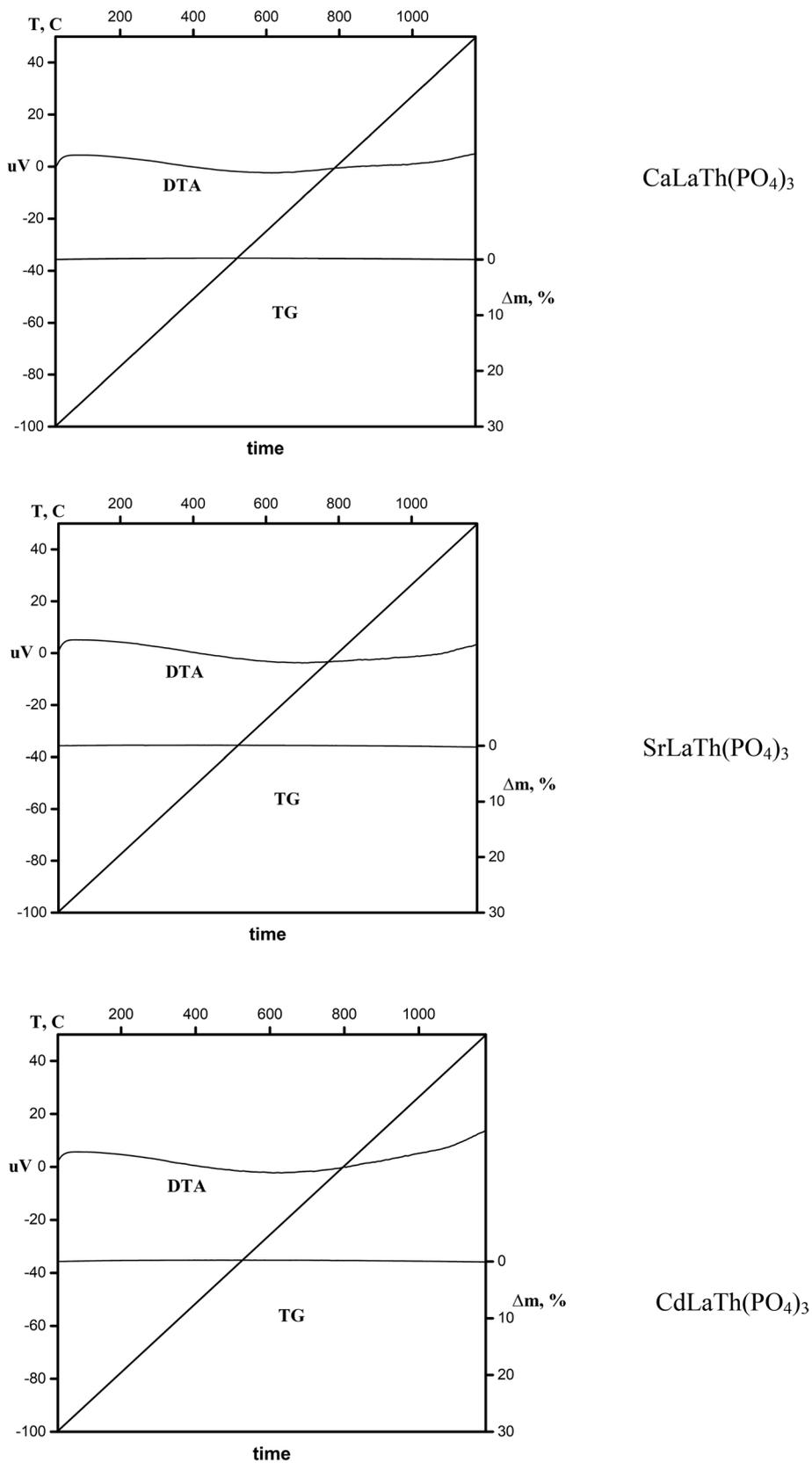
References

1. Lutze W, Ewing RS (eds) (1988) Radioactive waste forms for the future. North-Holland, Amsterdam, p 495
2. Povarennykh SA (1966) Crystal chemical studies of minerals. Naukova Dumka, Kiev, p 416 (in Russian)
3. Volkov YuF (1999) Radiokhimiya 41(2):161
4. Orlova AI, Kitaev DB, Kemenov DB (2003) Radiokhimiya 45(2):97
5. Lucuta PG, Verrall RA, Matzke H, Palmer BJ (1991) Microstructural features of SIMFUEL—simulated high-burnup UO2-based nuclear fuel. J Nucl Mater 178(1):48–60
5. Sazonov AA (2011) Sintez, stroyeniye i fiziko-khimicheskiye svoystva dvoynykh nitratov, fosfatov i vanadatov toriya [Synthesis, structure and physicochemical properties of thorium double nitrates, phosphates and vanadates]
6. Macrae CF, Edgington PR, McCabe P, Pidock E, Shields GP, Taylor R, Towler M, van de Streek J (2006) Mercury: visualization and analysis of crystal structures. J Appl Cryst 39:20 453–457.
7. Uvarov V (2019) The influence of X-ray diffraction pattern angular range on Rietveld refinement results used for quantitative analysis, crystallite size calculation and unit-cell parameter refinement. J Appl Cryst 52:252–261
8. Uvarov V (2019) Supporting Information for article: the influence of X-ray diffraction pattern angular range on rietveld refinement results used for quantitative analysis, crystallite size calculation and unit-cell parameter refinement. J Appl Cryst 52:252–261
9. Bruker (2006) TOPAS V3.0 user's manual. Bruker AXS, Karlsruhe
10. Hellenbrandt M (2004) The inorganic crystal structure database (ICSD)—present and future. Crystallogr Rev 10:17–22
12. Adelstein N, Mun BS, Ray HL, Ross PN Jr, Neaton JB, Jounghe LC (2011) Structure and electronic properties of cerium orthophosphate: theory and experiment. Phys Rev B 83:205104